JOURNAL OF GEOPHYSICAL RESEARCH, VOL. 105, NO. D19, PAGES 24,351–24,361, OCTOBER 16, 2000

Does cloud processing of aerosol enhance droplet concentrations?

Graham Feingold
NOAA Environmental Technology Laboratory, Boulder, Colorado

Sonia Kreidenweis
Department of Atmospheric Science, Colorado State University, Fort Collins

Abstract. In this paper we explore phase space for cloud processing of cloud condensation nuclei (CCN) via heterogeneous chemistry. A range of input CCN size spectra, parameterized as lognormal distributions, are used as input to a parcel model driven along trajectories derived from a large-eddy simulation of the stratocumulus-capped marine boundary layer. A simple sulfate chemistry model is coupled to the microphysical model. Gas phase concentrations of SO_2, O_3, H_2O_2, and NH_3 are varied so as to generate one case for which SO_2 processing is dominated by oxidation via O_3 and another case for which processing is dominated by oxidation via H_2O_2. The processed aerosol spectra are then used as input to an adiabatic parcel model that predicts the drop concentration for a given updraft velocity. Comparisons are made between predictions of drop concentration based on input of aerosol spectra that have experienced processing and an equivalent set that has not experienced processing. It is shown that for both of the chemical processing scenarios, heterogeneous processing can either enhance or suppress the number of drops activated in the subsequent cloud cycle, depending on the input CCN distribution and the magnitude of the updraft. Enhancement of drop concentration occurs in cases where the subsequent cloud cycle has low vertical velocity. A reduction in drop number occurs when updraft velocities in the subsequent cloud cycle are high. The size of the smallest CCN size category activated in the subsequent cloud cycle, relative to that experienced in the original cloud cycle, is important in determining the change in number of activated drops. By applying probability distribution functions of the vertical velocity, we calculate that, on average, drop concentrations are likely to be enhanced by between 10% and 20% for the cases examined. Nevertheless, the potential for both positive and negative changes in drop concentration due to cloud processing may complicate predictions of the indirect effect of aerosols on climate.

1. Introduction

The term aerosol "direct effect" has been coined to describe the climatic implications for the interaction of solar radiation with aerosol particles [e.g., *Charlson et al*., 1992]. Some fraction of the aerosol population is hygroscopic, and at sufficiently high relative humidity (>80%) these particles swell to sizes significantly larger than their dry sizes, thus affecting their interaction with solar radiation. Under the right conditions, cloud droplets may form on the hygroscopic particles, resulting in more dramatic increases in size and commensurate effects on radiation; the latter has been termed the "indirect effect" [*Twomey*, 1974]. Twomey hypothesized that increased concentrations of atmospheric aerosol will result in higher concentrations of cloud condensation nuclei (CCN) and increased cloud droplet concentrations. This chain of events will impact cloud microphysical processes. Higher droplet concentrations will suppress drizzle formation [*Albrecht*, 1989] and maintain larger liquid water paths and more reflective clouds.

Over the past decade, studies have determined that cloud processing of aerosol through heterogeneous chemistry can have a marked effect on the aerosol size distribution. Through this process, hygroscopic particles that have grown into cloud droplets are modified in size by the addition of nonvolatile mass that remains in the aerosol phase when the water is evaporated. One of the most studied examples is the addition of sulfate mass due to aqueous conversion of S(IV) to S(VI) [e.g., *Hoppel et al*., 1990; *Hegg et al*., 1996; *Bower and Choularton*, 1993; *Feingold et al*., 1998; *Zhang et al*., 1999] (*Zhang et al*. [1999] will hereinafter be referred to as Z99). Aerosol size spectra that have undergone cloud processing are characterized by bimodal spectra, with one mode of particles resulting from those that did not participate as CCN and a second mode in the region of 0.1-μm radius comprising those that were affected by processing. This process is important because it influences both the aerosol direct effect [*Hegg et al*., 1996], by generating particles that are efficient scatterers, and the indirect effect. *Bower and Choularton* [1993] presented results that showed that when aerosol spectra have undergone prior processing, there is an enhancement in drop concentration N in subsequent cloud cycles. Similar results were indicated by *Hegg et al*. [1996], although they contrasted a case with significant enhancement in CCN (at a specified supersaturation) with one where enhancement was small. The importance of this enhancement in drop number N lies in the fact that a cloud with

Paper number 2000JD900369.
0148-0227/00/2000JD900369$09.00

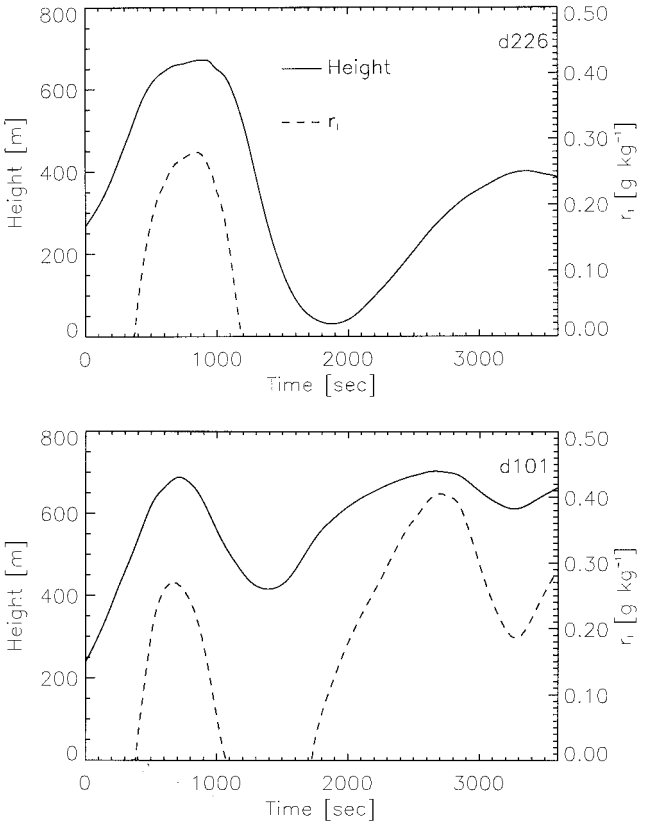

Figure 1. Time series of r_l and altitude for each of the parcel trajectories.

higher N will be more reflective (assuming the same water content) and will also be less apt to form precipitation. In warm clouds, larger precipitation-sized drops are formed by collection, a process that decreases drop concentrations and modifies cloud optical properties [*Feingold et al*., 1997, 1999a]. If significant amounts of water leave the cloud through precipitation, the effect on the cloud optical properties is even more profound.

In a recent paper, *Feingold et al*. [1998] (hereinafter referred to as F98) showed that heterogeneous processing of aerosol may not necessarily enhance the number of drops in subsequent cloud cycles. In that study an ensemble of 500 parcel trajectories was used to drive parcel models describing aerosol-cloud-aqueous chemistry interactions. For the aerosol size distribution used as input in that study, the number concentration of drops was not enhanced by processing. Moreover, the fact that processing had increased the size of some of the particles resulted in a slight enhancement in the growth of larger drops and precipitation formation.

It is apparent that the effect of aerosol/cloud processing on the next cloud cycle is not always in the direction of enhancing cloud reflectivity and inhibiting precipitation. The motivation for the present study is therefore to explore the conditions under which processing enhances or decreases the number concentration of drops. Instead of using a single aerosol size distribution as input to the model, we explore 125 different aerosol inputs to the model in the form of parameterized lognormal functions. To reduce computation time, only two of the 500 trajectories are selected for this study. Once a set of processed aerosol spectra has been generated, the individual spectra are then used as input to an adiabatic parcel model to explore the effects on activation and drop growth. By comparing simulations where processed spectra are used as input with simulations where unprocessed spectra are used as input, a measure of the percentage difference in droplet activation due to the processing is derived.

Table 1. Input Data for the Model

Input Parameter	Base (H_2O_2 Limited)	S1 (SO_2 Limited)
SO_2	2	2
H_2O_2	0.3	2.5
O_3	30	30
NH_3	1	1
HNO_3	0	0

Gas concentrations are in parts per billion by volume; however, the model uses the conservative mixing ratio units of mol g^{-1} (air).

2. Model

2.1. Coupled Microphysical/Chemistry Model

The modeling framework is described in detail by *Stevens et al*. [1996], F98, and Z99. Briefly, a large-eddy simulation (LES) of a stratocumulus-capped marine boundary layer is performed for a period of about 3 hours. During the course of the simulation, 500 parcel trajectories are tracked over the course of 1 hour and stored for later use. The ensemble of 500 parcels, or some subset thereof, is then used to drive individual parcel models that simulate coupled microphysics and heterogeneous chemistry. By simulating 500 parcels, one obtains a sense of the degree of variability that boundary-layer parcels are likely to encounter. Because the parcels are derived from the host LES, they are not necessarily adiabatic parcels, but instead reflect the local state of the boundary layer as simulated by the LES. F98 and Z99 ran 500 parcel model simulations on each of the stored trajectories. Their studies indicated that the details of the individual trajectories were not as important as the fact that they had similar mean in-cloud residence times and mean cloud liquid water mixing ratios r_l to those averaged from the ensemble of parcels. For this reason, only two of those parcels are selected in the current work. One has a mean in-cloud residence time of 14 min and a mean r_l of 0.18 g kg^{-1}, i.e., close to the ensemble mean, and is labeled d226; the other experiences two in-cloud sojourns and, overall, a longer in-cloud residence time and a higher mean r_l than the ensemble mean. It is labeled d101. Figure 1 indicates altitude and r_l time series for the two parcels.

Two different gas concentrations are used as input to the model; the first is considered the base case, and the second is considered sensitivity 1 (S1) as described by Z99 and in Table 1. No gas phase chemistry is considered here, so that gas depletion occurs only through dissolution into the aqueous

Table 2. Lognormal Input Parameters for the Model

N_a, cm^{-3}	r_g, μm	σ
100	0.03	1.5
500	0.04	1.6
1000	0.05	1.7
2000	0.06	1.8
5000	0.07	1.9

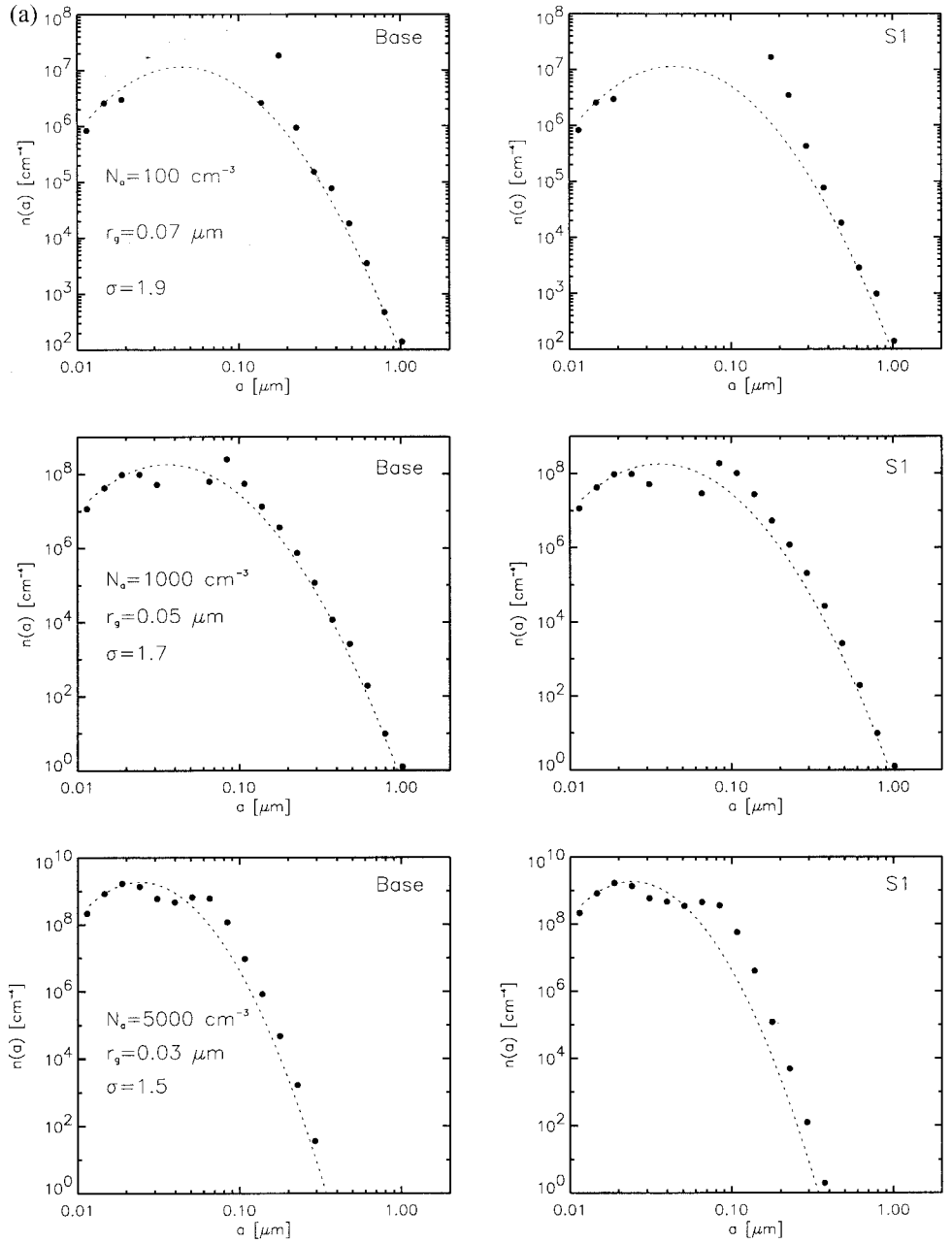

Figure 2. Comparisons of input and processed spectra for base and sensitivity 1 (S1) chemistry as well as for each of the trajectories (a) d226 and (b) d101.

phase and heterogeneous reaction. Further details are given by F98 and Z99.

The input aerosol is assumed to be a completely soluble ammonium sulfate aerosol; however, the heterogeneous chemistry processing changes the ratio of ammonium to sulfate ions (Z99). The size distributions are defined by a lognormal function prescribed over the size range 0.011–1.1 μm for particle radius a

$$n(a) = \frac{N_a}{\sqrt{2\pi}\,\ln\,\sigma a}\, e^{-\ln^2 (a/r_g)/(2\,\ln^2\,\sigma)}, \qquad (1)$$

where N_a is the total particle concentration, r_g is the median particle size, and σ is the geometric standard deviation. The range of these parameters is given in Table 2, yielding a total of 125 input spectra.

The spectrum is divided into 50 logarithmically increasing points on a mass grid, i.e., significantly higher resolution than the five points used by F98 and Z99. This was deemed necessary because the current study focuses on the number of activated droplets, and poor resolution produces a rather coarse step-like representation of activation. First, tests were performed to calculate the inherent error in the 50-point structure. The difference in drop activation resulting from the difference between any two adjacent grid points above the activation radius, relative to the total number activated, was shown to be $<3\%$. Errors tended to be smaller at smaller radii,

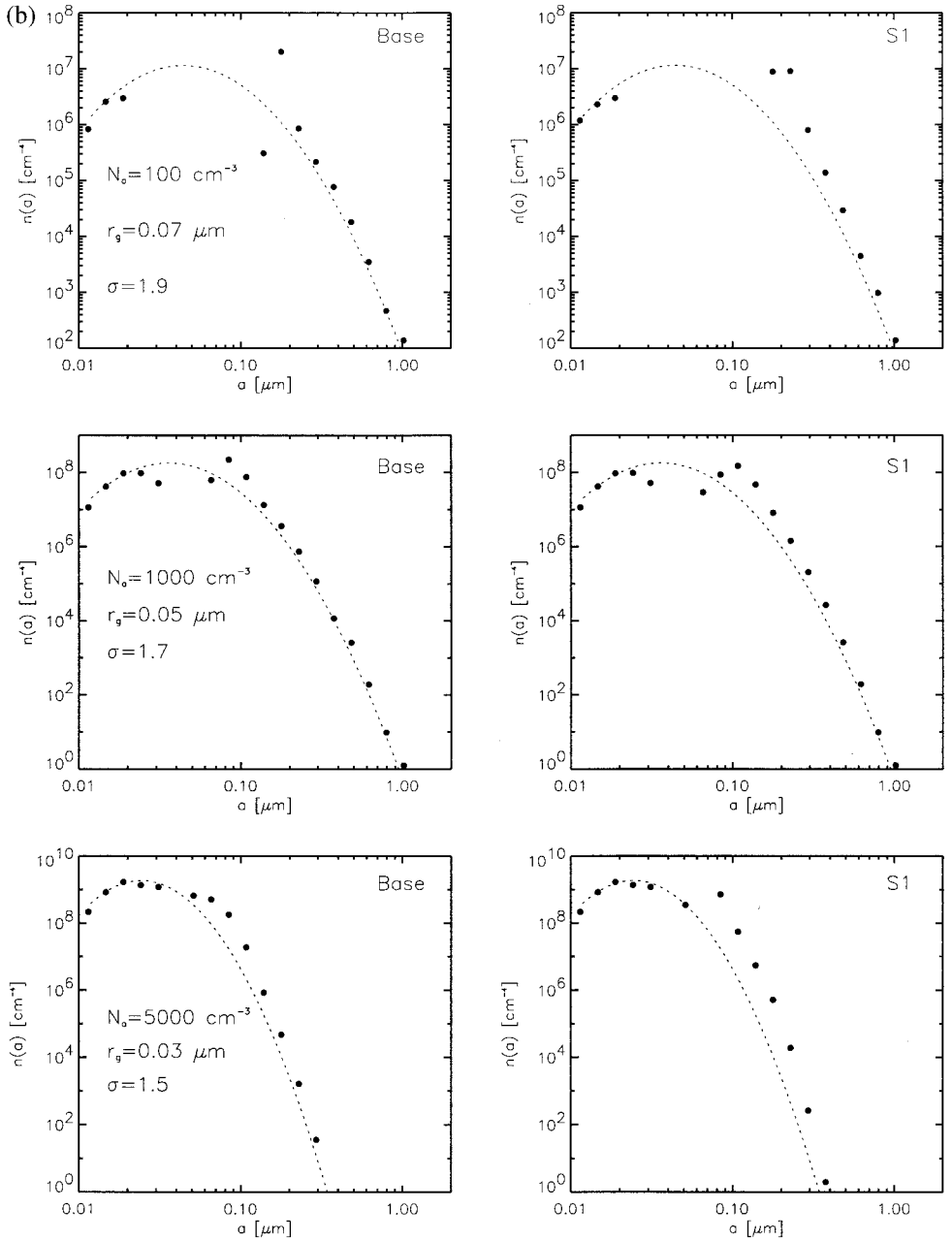

Figure 2. (continued)

where resolution is higher, and higher at larger radii, where resolution is lower. Second, tests with 20-point resolution showed small differences from the 50-point results. To be cautious, we opted for higher resolution.

The growth of the particles, as they accrete vapor or as they add mass due to sulfate formation, is calculated on a moving (Lagrangian) mass grid. At any time, the aerosol distribution, modified by heterogeneous chemistry, can be examined. If the parcel is still inside the cloud, this requires evaporating the existing water. Sample input and modified aerosol spectra are shown in Figure 2 for d226 and d101 as well as for the base case and S1. Spectra have been temporally averaged so as to provide a representative spectrum over a few minutes of processing. This was done by binning the individual spectra into a 25-bin structure. The characteristic separation of the spectrum into two modes is seen in all plots, with the details determined by the initial size distribution of aerosol and the nature of processing. When the number concentration of particles is small, the effect of processing is most pronounced, since the same amount of sulfate mass is spread over fewer particles. Also, processed spectra in the S1 case tend to show more processing of the larger particles than the equivalent base runs. Z99 showed that in S1, where oxidation is predominantly through the H_2O_2 pathway and therefore independent of pH, mass is added more evenly across the size distribution, whereas in the base case (dominated by O_3 oxidation), most of the mass is added to particles where dilution has maintained a pH above about 5.

2.2. Adiabatic Parcel Model

The methodology adopted is to consider both unprocessed (lognormal) and processed CCN spectra as input to a model

representing a single subsequent cloud cycle. An adiabatic parcel model (APM) that represents the hygroscopic growth of the CCN and droplet condensation (but not heterogeneous chemistry) [*Feingold and Heymsfield*, 1992] is used for this purpose. The APM is used to determine drop concentration N as the response to a given aerosol size spectrum in an adiabatic updraft with prescribed vertical velocity. By comparing the response to processed spectra with the response to original unprocessed spectra with the same total particle concentration, a measure of the effect of processing on drop activation can be determined. This is a convenient way of estimating the sign and magnitude of the impact, although a number of caveats are in order. (1) The APM is not as realistic a representation of real clouds as, for example, the LES. F98 used a processed and unprocessed spectrum as input to the LES and showed that for that given CCN spectrum, processing resulted in a similar number of activated drops. The difficulty of using the LES for these exercises is that it does not represent droplet growth and activation as accurately as the APM, and in addition, it requires enormous computation time for each simulation, thus limiting the amount of phase space that can be covered. (2) Using the APM approach, only one subsequent updraft is investigated, while clearly natural clouds would experience many of these cycles.

A number of different experiments have been performed. For both base and S1 chemistry, as well as for trajectories d226 and d101, the 125 CCN spectra indicated in Table 2, together with their processed counterparts, are input to the APM at seven different updraft velocities, namely, $w = 20$, 50, 75, 100, 150, 200, and 300 cm s^{-1}. This yields a total of 875 APM runs for each of the simulations, i.e., 875 runs for the unprocessed case, as well as for each of d101 (base), d101 (S1), d226 (base), and d226 (S1).

3. Results

3.1. Ensemble Results for Base Case and d226

Figure 3 compares the cloud drop concentrations, defined as all drops with radii larger than 1 μm, for the base case (d226) with those for the unprocessed case. The percentage difference is calculated as

$$\delta N = 100\,\frac{N_p - N_{up}}{N_{up}}, \tag{2}$$

where N_p and N_{up} are the drop number concentrations for the processed and unprocessed cases, respectively, calculated when N reaches a maximum in the APM. Note that δN varies over a range of about -30% to 150%, and although the positive δN are considerably larger than the negative δN, there are frequent occurrences of negative δN (135 data points for $\delta N < -5\%$ and 202 points for $\delta N > 5\%$). The systematic decrease in δN observed in Figure 3 is related to the sequence of the simulations, and the reasons for this are now explored. It is apparent that there is no strong systematic change in δN with either r_g or σ (Figure 4), with both positive and negative δN occurring at all r_g and σ. At small r_g the maximum positive δN is as high as 120%, whereas at large r_g, the maximum positive δN is no greater than 50%. The smallest δN seem to occur at the highest N_a, and the largest δN occur when N_a is between about 500 and 2000 cm^{-3}. The clearest result is the general decrease in δN with increasing updraft velocity w, and in fact because the sequence of simulations in Figure 3 was from smaller w to larger w, these two figures are somewhat comparable.

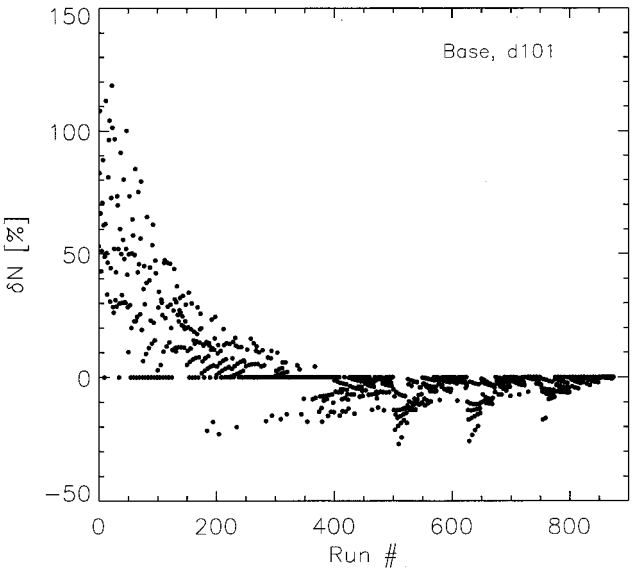

Figure 3. Percentage change in N in a subsequent cloud cycle as a result of processing. Here δN is derived from the difference between the number of activated droplets produced by the adiabatic parcel model for unprocessed and processed spectra. A total of 875 simulations were performed for the range of aerosol size spectra in Table 2 and for vertical velocities of $w = 20$, 50, 75, 100, 150, 200, and 300 cm s^{-1}.

In order to explore the dependence of δN on w we consider the definition of drop number N:

$$N = \int_{r_{\rm cut}}^{r_{\rm max}} n(a)\,da, \tag{3}$$

where $r_{\rm cut}$ is the size of the smallest activated CCN and $r_{\rm max}$ is the maximum particle radius. (Strictly speaking, particles are activated when they have grown beyond the critical radius determined by Köhler theory. This definition includes most small particles but excludes large particles that seldom attain their equilibrium sizes but are nevertheless large enough to participate in cloud microphysical processes. Therefore the term "activated" is used here in the sense that the CCN have grown to sizes typical of cloud droplets, i.e., > about 1 μm radius.) The cutoff radius $r_{\rm cut}$ can be calculated from simple formulae [e.g., *Pruppacher and Klett*, 1997] or directly from the model data. Note that w, $S_{\rm max}$, and $r_{\rm cut}$ are not independent parameters and are intimately related to one another; for example, larger w are associated with larger $S_{\rm max}$ and smaller $r_{\rm cut}$. Figure 5 plots $S_{\rm max}$ for the processed cases versus $S_{\rm max}$ for the unprocessed cases. In all cases, the effect of processing is to diminish the value of $S_{\rm max}$, regardless of the CCN input or the magnitude of w. The processed particles are larger, their Köhler curves are displaced to larger radii and lower supersaturations, and they are therefore more efficient at taking up vapor and grow more readily. Because processing diminishes $S_{\rm max}$, $r_{\rm cut}$ for the processed case is always larger than $r_{\rm cut}$ for the unprocessed case.

We now define three different $r_{\rm cut}$ parameters. The first, $r_{\rm cut(0)}$, pertains to the coupled microphysics/chemistry model responsible for the processing and is related to the dynamics of

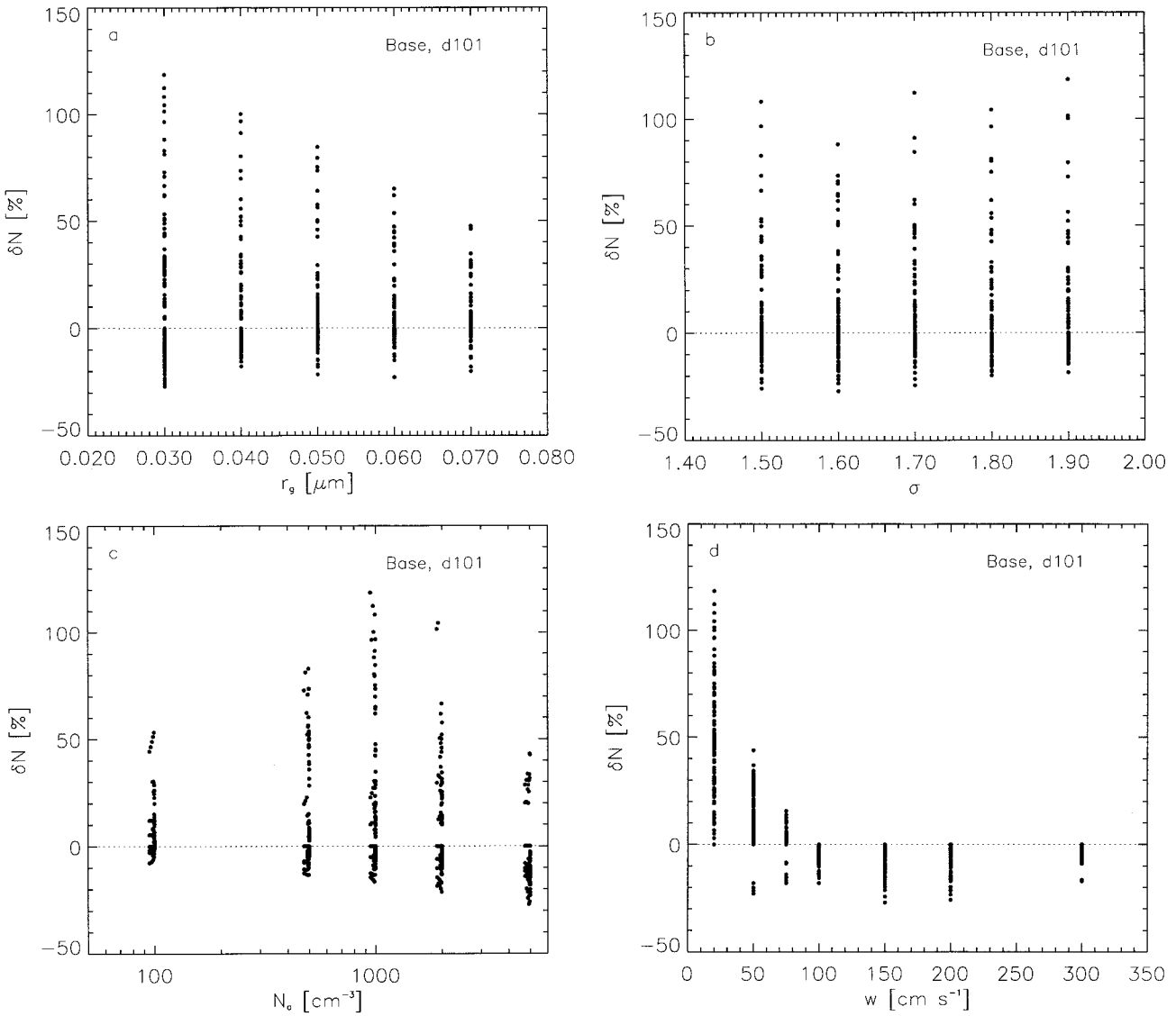

Figure 4. The δN sorted as a function of (a) r_g, (b) σ, (c) N_a, and (d) w for the simulations in Figure 3.

the LES-derived trajectory. The second, $r_{\mathrm{cut}(up)}$, pertains to the unprocessed lognormal spectra used as input to the APM; the third, $r_{\mathrm{cut}(p)}$, pertains to the processed spectra (the output spectra from the microphysics/chemistry model) that are input to the APM. The relative positions of these cutoff radii are illustrated in Figure 6.

At small w, only the larger particles are activated, and since this is the region that experiences a large local increase in N_a through the growth of smaller CCN, δN tends to be positive in spite of the fact that $r_{\mathrm{cut}(p)} > r_{\mathrm{cut}(up)}$. As w increases, increasingly smaller particles can be activated, and if w is large enough, r_{cut} is located where there is no difference between the unprocessed and processed spectra ($r < r_{\mathrm{cut}(0)}$). Bearing in mind that processing changes only the sizes of particles but not their total number concentration, the fact that $r_{\mathrm{cut}(p)} > r_{\mathrm{cut}(up)}$ translates to a decrease in the number of activated drops when $r < r_{\mathrm{cut}(0)}$. This is discussed further in section 4.

In Figure 7a, δN is plotted as a function of $r_{\mathrm{cut}(p)}/r_{\mathrm{cut}(0)}$. A fairly distinct threshold between $+\delta N$ and $-\delta N$ is seen at $r_{\mathrm{cut}(p)}/r_{\mathrm{cut}(0)} \approx 1$. When the δN data are plotted in $r_{\mathrm{cut}(p)}/r_{\mathrm{cut}(0)}$, w phase space (Figure 7b), it can be seen that there is a clustering of $+\delta N$ toward larger $r_{\mathrm{cut}(p)}/r_{\mathrm{cut}(0)}$ and smaller w, while $-\delta N$ points exist at $r_{\mathrm{cut}(p)}/r_{\mathrm{cut}(0)} < 1$ and higher w. As will be seen in section 4, these results are consistent for the S1 chemistry and for trajectory d101.

3.2. Some Individual Results

In order to focus on the processes responsible for the sign of δN, two individual cases are examined more closely. These were chosen at random from the base chemistry, d226 experiments discussed above. A number of other cases were analyzed, and all showed patterns similar to those in the following discussion. The first case is for the input CCN spectrum $N_a = 500\ \mathrm{cm}^{-3}$, $r_g = 0.07\ \mu\mathrm{m}$, and $\sigma = 1.7$. The unprocessed and processed spectra yield $\delta N = 24\%$ when input to the APM at $w = 20\ \mathrm{cm\ s}^{-1}$. The second case is for the input CCN spectrum $N_a = 2000\ \mathrm{cm}^{-3}$, $r_g = 0.04\ \mu\mathrm{m}$, and $\sigma = 1.8$, which produces $\delta N = -11\%$ at $w = 200\ \mathrm{cm\ s}^{-1}$.

Time series of the microphysical fields of r_l, N, effective radius r_e, and supersaturation S are shown in Figure 8 for each of these cases. Note that in both cases, r_l increases linearly with time (equivalent to height) and the effect of processing on the

r_l field is negligible. Processing causes a rapid and sustained rise in N for the $\delta N = 24\%$ case, despite the fact that S is lower. The result is a distinct decrease in r_e equivalent to approximately one third of the percentage increase in drop number ($\delta r_e/r_e \approx -1/3 \times \delta N/N$ for constant r_l), with any deviations due to differences in the drop spectral breadth. When $\delta N = -11\%$, a different picture emerges. Processing results in premature growth of large particles to supermicron sizes at about 105–110 s. However, the activation of smaller particles cannot be sustained, especially because S is lower, and falls behind the unprocessed case. It is interesting to note that the step-like nature of N is such that had the processed and unprocessed cases been compared at $S_{\max}$ rather than at $r_l = 0.5$ g kg^{-1}, δN would not have been as meaningful. An r_l smaller than 0.5 g kg^{-1} but far enough away from $S_{\max}$ would have been sufficient for a representative calculation of δN, but since $r_l = 0.5$ g kg^{-1} is quite typical of stratocumulus or small nonprecipitating cumulus, we opted to compare results at this threshold.

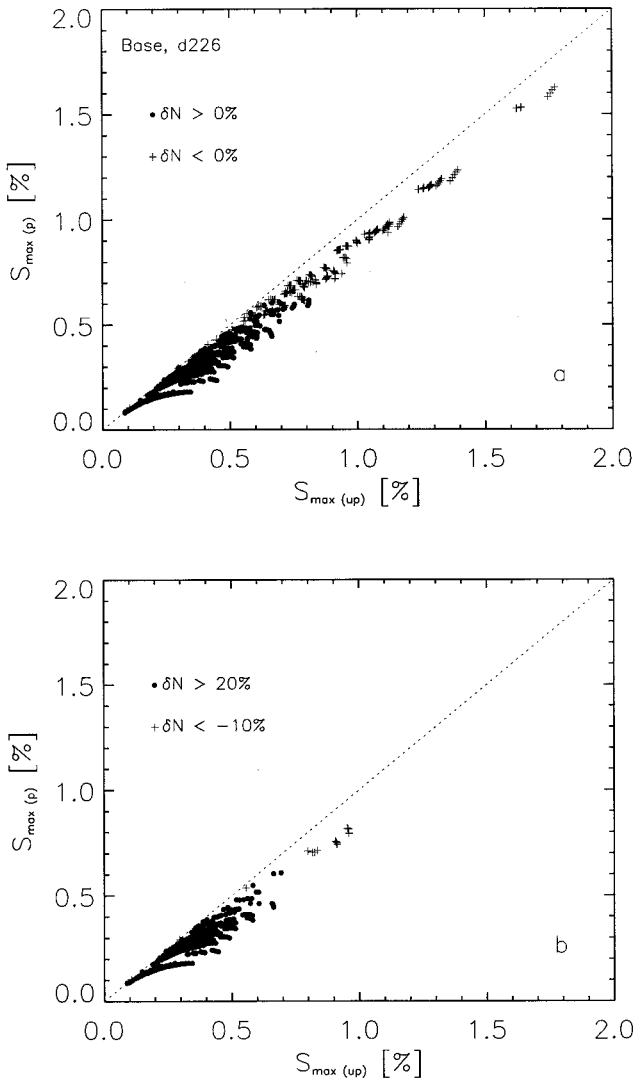

Figure 5. $S_{\max}$ produced by the adiabatic parcel model (APM) for processed spectra versus those produced by the APM for unprocessed spectra. (a) All data sorted by the sign of δN. (b) Data sorted for $\delta N > 20\%$ and $\delta N < -10\%$.

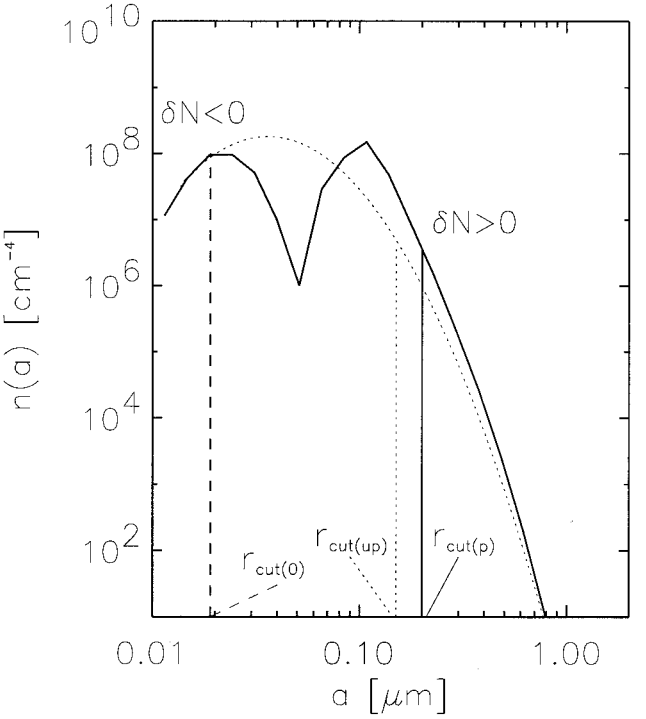

Figure 6. Schematic of an unprocessed and processed aerosol size spectrum showing the relative positions of $r_{\text{cut}(p)}$ and $r_{\text{cut}(up)}$, as well as the $-\delta N$ and $+\delta N$ regimes. The $-\delta N$ regime lies in the region $r_{\text{cut}(p)} < r_{\text{cut}(0)}$. See text for discussion.

4. Discussion and Sensitivity Tests

Figure 6 is a schematic representation of a processed and unprocessed aerosol spectrum showing the $-\delta N$ and $+\delta N$ regimes as well as the relative positions of r_{cut} parameters and serves to summarize the following discussion. In general, we have seen that processed spectra, when input into the APM, generate lower $S_{\max}$ than for the unprocessed lognormal regardless of w (Figure 5). This means that $r_{\text{cut}(p)}$ is always $> r_{\text{cut}(up)}$. Despite this, there is a general enhancement in N at low $S_{\max}$ because the difference in r_{cut} does not make up for the fact that the area under the processed spectrum for $r > r_{\text{cut}(p)}$ is so much larger due to the local increase in the number of particles that have grown into this range by chemical processing (Figure 6). However, as one gets to the highest $S_{\max}$ (or lowest r_{cut}), the fact that $S_{\max}$ for the processed case is smaller than that for the unprocessed case, dominates. At these high S we are entering the regime where the spectra are quite similar. Therefore lower S translates quite simply to smaller N, i.e., $-\delta N$. Figure 7 is an alternative but equivalent way of demonstrating this result.

It is noteworthy that the minimum negative δN do not occur where w, and therefore S, are largest but in some intermediate zone (Figure 5). Analysis has shown that the minimum δN occur where processing has created a local dearth of particles, which we will refer to as the "gap." This gap exists because of the separation of the two modes due to processing and is most pronounced at low aerosol number concentrations (Figure 2).

In nature the gap may be at least partially filled, as many different spectra that have each experienced different processing histories are mixed. Nevertheless, to explain the current

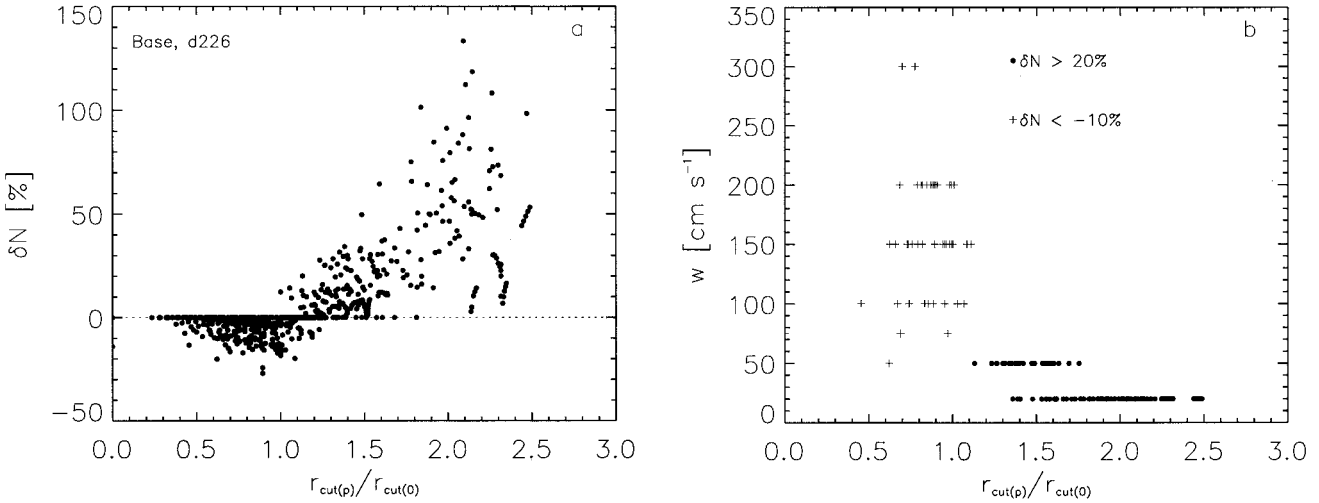

Figure 7. (a) The δN as a function of the ratio of r_{cut} parameters. Here $r_{cut(p)}$ is the smallest particle radius activated when the processed spectrum is used as input to the APM, and $r_{cut(0)}$ is the smallest particle radius activated in the trajectory model. (b) Vertical velocity w in the APM as a function of the ratio of the r_{cut} parameters defined in Figure 7a.

results, one must consider that in this region, increases in S do not translate to increases in N because there are simply no (or few) new particles to activate. For the unprocessed lognormal spectra, on the other hand, an increase in S translates directly to higher N because the particles maintain their original logarithmic spacing.

4.1. Ensemble Results for Different Chemistry and/or Trajectories

Figure 9 repeats calculations displayed in Figure 7 for d226, S1 chemistry; d101, base chemistry; and d101, S1 chemistry. In all cases it is seen that there is qualitative agreement in the dependence of δN on $r_{cut(p)}/r_{cut(0)}$. Because the behavior of δN for d101 and base chemistry is qualitatively similar to other trajectories and chemical processing scenarios, we conclude that the results are robust.

4.2. Averaging Based on PDFs of w

The results consistently show a strong dependence of δN on w. In the numerical experiments described here, a fixed w is used to describe individual activation events in the APM. However, the boundary layer is more realistically represented by a probability distribution function (PDF) of vertical velocities. PDFs are sometimes approximated by Gaussian distributions, but they can also be derived from remote sensors [*Frisch et al.*, 1995] or estimated from numerical models. The base-case results are now averaged by weighting δN by the PDF of w for (1) the cloud base PDF of w derived from the LES described in section 2.1, and (2) assumed Gaussian PDFs of w with mean $w = 0$ and three different variance parameters, $\sigma_w^2 = 0.5$, 1.0, and 1.4 m^2 s^{-2}:

$$\overline{\delta N}(N_a, r_g, \sigma) = \int_{w>0} \delta N(N_a, r_g, \sigma, w) f(w)\, dw. \quad (4)$$

Figure 10 shows the values of $\overline{\delta N}(N_a, r_g, \sigma)$ for the four different PDF weightings. The lowest value of $\sigma_w^2 = 0.24$ is derived from the LES. It is clear that because of the low frequency of occurrence of large w, $\overline{\delta N}$ is, on average, positive and of the order of 10–20%. Nevertheless, at any given σ_w^2, there is a broad range of $\overline{\delta N}$ depending on the aerosol size spectrum. As expected, the mean $\overline{\delta N}$ (averaged over all spectra) decrease with increasing variance of the PDF, i.e., as higher w become more frequent. The extent to which these PDFs are relevant to cloud activation probably depends on cloud type. The cloud processing simulated here has been calculated within a marine stratocumulus environment, so subsequent cloud cycles are likely to be of a similar kind. Thus for stratus or stratocumulus clouds, the PDF weighting such as the one derived from the LES stratocumulus simulation may be quite appropriate. However, if subsequent cloud cycles are convective cumulus clouds (e.g., as stratocumulus decks move over warmer waters, they become more cumulus-like), the higher w may be more relevant and therefore underrepresented in the PDF-weighted analysis. (In convectively unstable atmospheres, clouds are more likely to form above vigorous updrafts.)

4.3. Implications for Radiative Effects

The implications of heterogeneous processing of aerosol for radiative effects are twofold. First, the particles of the order of 0.1-μm radius generated by heterogeneous processing are very efficient scatterers in the visible, and therefore their direct effect is considerable [*Hegg et al.*, 1996]. The implications for the indirect effect are less easily defined. Enhancement in drop number concentration will tend to generate clouds that are more reflective and less apt to precipitate. Their enhanced lifetimes will increase the amount of processing that occurs, provided there are ample sources of SO_2 and oxidants. If all other conditions are equal, this might imply a positive feedback process that produces brighter and more colloidally stable clouds. However, it is intuitive that this process will likely reach saturation. The fact that precipitation does occur intermittently in marine boundary layers suggests that this cycle is broken at some point. We have seen here that δN is negative when w is high, and therefore periodic vigorous updrafts may cause a decrease in drop number. These more vigorous clouds will penetrate higher and generate more liquid water [*Feingold*

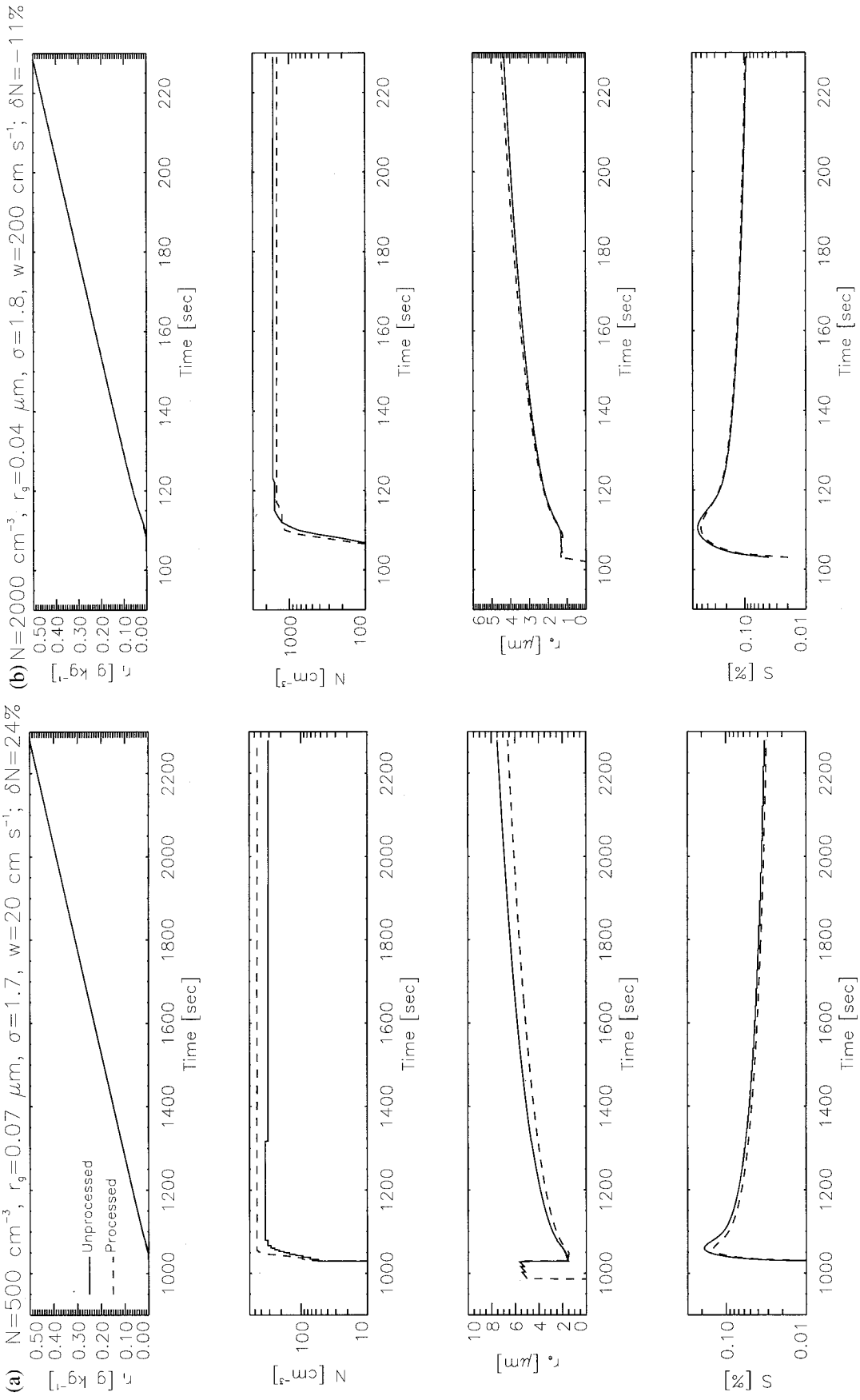

Figure 8. Time series of cloud water mixing ratio r_l, number of activated drops N, drop effective radius r_e, and supersaturation S for individual APM runs for a case where (a) $\delta N = 24\%$ and (b) $\delta N = -11\%$. The solid lines indicate results for unprocessed spectra input to the APM; the dashed lines are for processed spectra input to the APM.

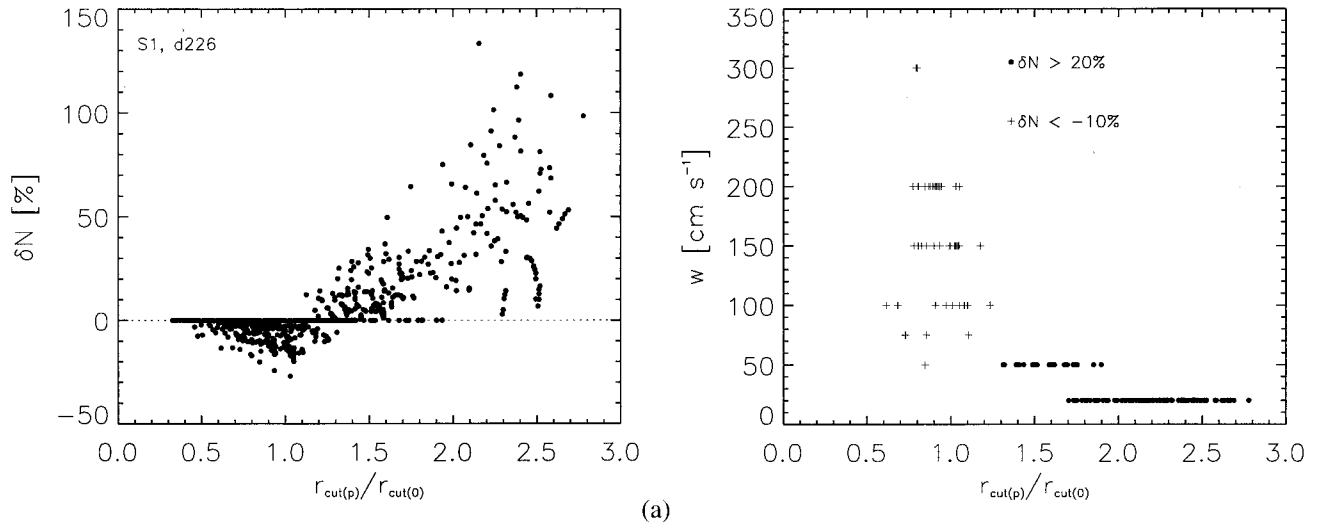

Figure 9. Same as in Figure 7 but for (a) trajectory d226 and S1 chemistry, (b) trajectory d101 and base chemistry, and (c) trajectory d101 and S1 chemistry.

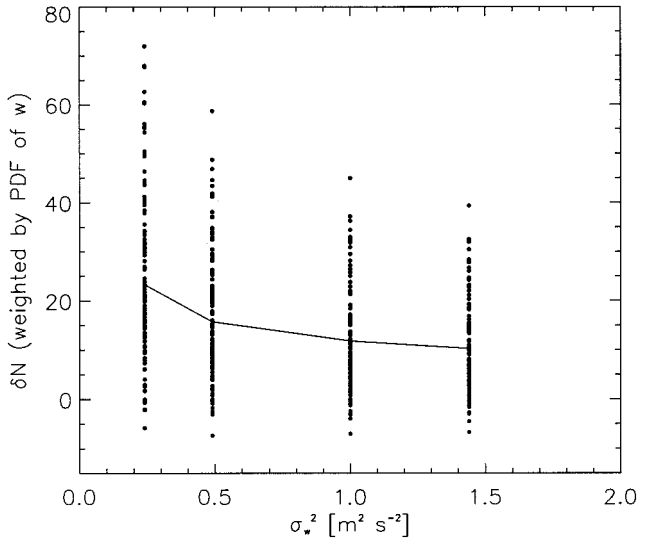

Figure 10. Values of δN weighted by the probability distribution function (PDF) of vertical velocity as calculated in equation (4) as a function of vertical velocity variance σ_w^2. At any given σ_w^2, variability is due to the aerosol spectral parameters N_a, r_g, and σ. The leftmost set of points pertains to the PDF derived from the large-eddy simulation (just above cloud base). The other sets of points pertain to assumed Gaussian PDFs with mean $w = 0$ and σ_w^2 as indicated. The solid line connects the mean values.

et al., 1999b], thereby further increasing the chances of a reduction in N as collision-coalescence ensues. Wetter clouds are more likely to precipitate, so all these factors work in unison.

Another mechanism for breaking the cycle of increasing N is the presence of a sufficiently strong background of giant CCN particles emitted by the ocean or transported from afar. *Feingold et al*. [1999a] showed that concentrations of giant CCN of 10^{-3} cm^{-3} are sufficient to generate collision-coalescence in stratocumulus at background CCN concentrations of up to 250 cm^{-3} and r_l of about 0.5 g kg^{-1}. Giant CCN may therefore provide another important regulating role in this process.

5. Summary

This study has explored cloud processing of aerosol through heterogeneous chemistry and its potential effect on cloud microphysics in subsequent cloud cycles. The motivation for this study lies in the possibility that processing might modify the reflectance of clouds by increasing the number of cloud drops N as proposed by *Bower and Choularton* [1993] and *Hegg et al*. [1996]. To investigate this phenomenon as thoroughly as possible, a broad range of aerosol size spectra and updraft velocities has been examined. It has been confirmed that under certain conditions, primarily low updraft velocities in the subsequent cloud, a processed aerosol spectrum does indeed produce an increase in N. However, it has also been shown that processing frequently results in a decrease in N, although these decreases tend to be more modest than the enhancements in N. The decreases in N are interesting in that they occur in spite of the increase in sulfate mass due to the processing and point to the importance of the distribution of this mass with respect to aerosol size.

Because a typical boundary-layer probability distribution function of (positive) vertical velocities is such that lower vertical velocities are more frequent, the overall result of processing is expected to be an enhancement in N. The sequence of processing cycles and the multitude of scenarios that can be encountered in the boundary layer will likely affect the degree of this enhancement. Bearing in mind that the relative decrease in drop effective radius r_e is approximately one third of the relative increase in N, the fact that negative δN are so frequent, even at w as low as 50 cm s^{-1}, suggests that impacts on cloud radiative properties may be less than previously suggested.

Acknowledgments. The authors acknowledge funding from the NOAA Office of Global Programs under contract NA67RJ0152.

References

Albrecht, B. A., Aerosols, cloud microphysics, and fractional cloudiness, *Science*, *245*, 1227–1230, 1989.

Bower, K. N., and T. W. Choularton, Cloud processing of the cloud condensation nucleus spectrum and its climatological consequences, *Q. J. R. Meteorol. Soc*., *119*, 655–679, 1993.

Charlson, R. J., S. E. Schwartz, J. M. Hales, R. D. Cess, J. A. Coakley Jr., J. E. Hansen, and D. J. Hofmann, Climate forcing by anthropogenic aerosols, *Science*, *255*, 423–430, 1992.

Feingold, G., and A. J. Heymsfield, Parameterizations of condensational growth of droplets for use in general circulation models, *J. Atmos. Sci*., *49*, 2325–2342, 1992.

Feingold, G., R. Boers, B. Stevens, and W. R. Cotton, A modeling study of the effect of drizzle on cloud optical depth and susceptibility, *J. Geophys. Res*., *102*, 13,527–13,534, 1997.

Feingold, G., S. M. Kreidenweis, and Y. Zhang, Stratocumulus processing of gases and cloud condensation nuclei, 1, Trajectory ensemble model, *J. Geophys. Res*., *103*, 19,527–19,542, 1998.

Feingold, G., W. R. Cotton, S. M. Kreidenweis, and J. T. Davis, Impact of giant cloud condensation nuclei on drizzle formation in marine stratocumulus: Implications for cloud radiative properties, *J. Atmos. Sci*., *56*, 4100–4117, 1999a.

Feingold, G., A. S. Frisch, B. Stevens, and W. R. Cotton, On the relationship among cloud turbulence, droplet formation, and drizzle as viewed by Doppler radar, microwave radiometer, and lidar, *J. Geophys. Res*., *104*, 22,195–22,203, 1999b.

Frisch, A. S., D. H. Lenschow, C. W. Fairall, W. H. Schubert, and J. S. Gibson, Doppler radar measurements of turbulence in marine stratiform cloud during ASTEX, *J. Atmos. Sci*., *52*, 2800–2808, 1995.

Hegg, D. A., R. Majeed, P. F. Yuen, M. B. Baker, and T. V. Larson, The impacts of SO_2 oxidation in cloud drops and in haze particles on aerosol light scattering and CCN activity, *Geophys. Res. Lett*., *23*, 2613–2616, 1996.

Hoppel, W. A., J. W. Fitzgerald, G. M. Frick, and R. E. Larson, Aerosol size distributions and optical properties found in the marine boundary layer over the Atlantic Ocean, *J. Geophys. Res*., *95*, 3659–3686, 1990.

Pruppacher, H. R., and J. D. Klett, *Microphysics of Clouds and Precipitation*, 954 pp., Kluwer Acad., Norwell, Mass., 1997.

Stevens, B., G. Feingold, W. R. Cotton, and R. L. Walko, On elements of the microphysical structure of numerically simulated stratocumulus, *J. Atmos. Sci*., *53*, 980–1006, 1996.

Twomey, S., Pollution and the planetary albedo, *Atmos. Environ*., *8*, 1251–1256, 1974.

Zhang, Y., S. M. Kreidenweis, and G. Feingold, Stratocumulus processing of gases and cloud condensation nuclei, 2, Chemistry sensitivity analysis, *J. Geophys. Res*., *104*, 16,061–16,080, 1999.

G. Feingold, NOAA Environmental Technology Laboratory, 325 Broadway, Boulder, CO 80305. (gfeingold@etl.noaa.gov)

S. Kreidenweis, Department of Atmospheric Science, Colorado State University, Fort Collins, CO 80523.

(Received December 9, 1999; revised May 15, 2000;
accepted June 2, 2000.)